Electronic Supplementary Information (ESI)

Gas-Driven Exfoliation for Producing High-Quality Graphene

Zhiliang Zhang[a*], Hailun Jin[a], Xinfeng Miao[a], Ting Ju[a], Yang Li[a] and Jianbing Ji[a,b]

[a] College of Chemical Engineering, Zhejiang University of Technology, Hangzhou 310014, China

[b] Zhejiang Province Key Laboratory of Biofuel, Biodiesel Laboratory of China Petroleum and Chemical Industry Federation, Zhejiang University of Technology, Hangzhou 310014, China

*Corresponding authors.

Tel: +86-571-88320043, E-mail: zhangzl@zjut.edu.cn (Zhiliang Zhang)

Experimental details

Fig. 1S shows a flow diagram of the gas-driven exfoliation process. In a typical experiment, 4 g of the bulk graphite (Aladdin, Shanghai, ≥325 mesh, purity 99.9%; to remove the possible larger particles, the bulk graphite was sieved by a 325-mesh sieve) was firstly dispersed in 100 mL N-methylpyrrolidone (NMP) (Aladdin, Shanghai, purity 99.5%) by magnetic stirring (500 rpm, 10 min) to obtain graphite suspension with an initial concentration of 40 mg mL^{-1}. Next, the graphite suspension was pumped (flow rate: 15 L h^{-1}) by a plunger pump (2J-XZ, Zhijiang Petrochemical Co. Ltd, Hangzhou, China) to mix with compressed air (flow rate 550 L h^{-1}, 0.5 MPa) in a tee and then driven by high-speed gas to leave a 0.5-meter-long pipe (φ 3×1 mm). After that, gas in the gas-suspension mixture was separated by a cyclone separator and discharged into the atmosphere, while the suspension was collected and recycled. With multiple exfoliation cycling for 90 min, the suspension was centrifuged at 500 rpm for 1 h (SC-3610) to remove the unexfoliated graphite. Finally, the supernatant graphene dispersion was decanted and retained for further characterization.

The morphology and length of the bulk graphite and the gas-driven exfoliated graphene were observed by scanning electron microscopy (SEM) using a HitachiS-4700Ⅱ (Hitachi). Transmission electron microscopy (TEM) and high-resolution TEM (HR-TEM) images were captured using a Tecnai G2 F30 S-Twin (operated at 300 kV). The samples for TEM observation were prepared by drop casting the graphene dispersion onto holey carbon grids. Atomic force microscopy (AFM) analysis were performed in tapping mode by a Bruker Dimension Icon, and a newly cleaved mica was used as substrate. The samples for AFM analysis were prepared by dropping the NMP-diluted graphene dispersions (using a micro-syringe) onto the newly cleaved mica and drying in vacuum drying oven. Raman spectra was obtained by a Lab RAM HR800 Raman spectrometer with 532 nm laser excitation. X-ray photoelectron spectroscopy (XPS) was conducted by a ESCALAB 250Xi analyzer. UV-vis absorption was performed to measure graphene concentration by a Lambda 35 spectrophotometer (PerkinElmer) at a wavelength of 660 nm.

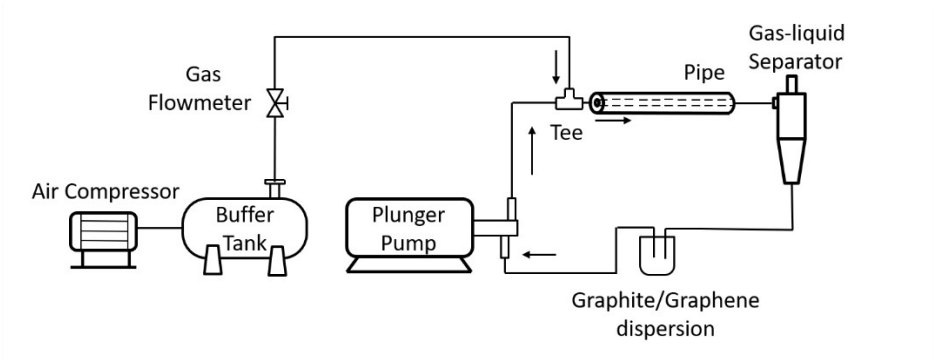

Fig. 1S. Schematic diagram of the gas-driven exfoliation process.

Exfoliation mechanism

Sheer rate in the pipe

The energy dissipation rate ε (per unit mass, m^2/s^3) inside the pipe is [1, 2]

$$\varepsilon = \frac{Q\Delta p}{m} \tag{1}$$

where Q is the volume of the gas inside the pipe; Δp is the pressure losses inside the pipe; m is the mass of the liquid inside the pipe. For $Q = 1.67\times10^{-4}$ m^3/s, $\Delta p = 0.5$ MPa, and $m = 6.94\times10^{-5}$ kg (φ 3×1 mm, 0.5 m), we get $\varepsilon = 1.2\times10^{6}$ m^2/s^3.

The sheer rate (γ) can be written as [3]

$$\gamma = \sqrt{\frac{\varepsilon}{\nu}} \tag{2}$$

where v is the kinematic viscosity, and it was estimated to be $v = \sim1\times10^{-6}$ m^2/s.

From eq. 2, the sheer rate in the pipe was calculated to be $\gamma = 1.1\times10^{6}$ s^{-1}.

Sheer rate at the inner edge of outlet

Considering the fact that liquid becomes a radial jet (-15° to15°) when it leaves the pipe (Fig. 2S (a)), the effective contact width (L) between liquid and the inner edge was estimated to be 1/6 of the width of the inner edge W (Fig. 2S (b)). The width of the inner edge was determined by SEM (Fig. 3S (b)) and measured to be ~10 μm.

The bending radius (R) of the effective contact width between liquid and the inner edge can be written as

$$R = \frac{180L}{n\pi} \tag{3}$$

where n is central angle. For L =1/6W=1.67 μm, and let n = 90°, we get R=1.06×10^{-6} m.

The sheer rate at the inner can be estimated by

$$\gamma \approx \frac{u}{R} \tag{4}$$

where u is the velocity of liquid at the outlet, which was measured to be 35 m s^{-1} by a high-speed camera (FASTCAM SA-X2 type 200K, Photron).

From eq. 4, the sheer rate at the inner edge was calculated to be γ = 3.3×10^{7} s^{-1}.

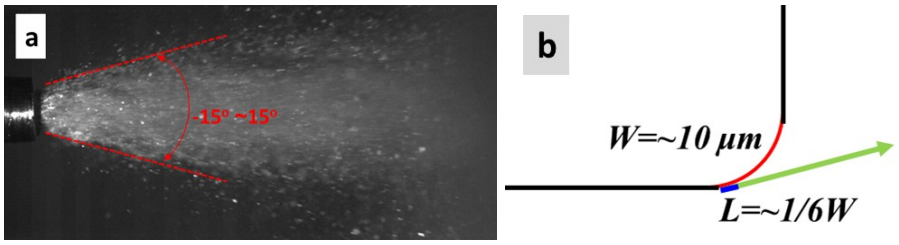

Fig. 2S. (a) High-speed camera photo of liquid leaving the pipe, and (b) a schematic view of the inner edge of outlet. The width of the inner edge W (red line) was measured to be 10 μm. The effective contact width L (blue line) between liquid and the inner edge was estimated to be 1/6W.

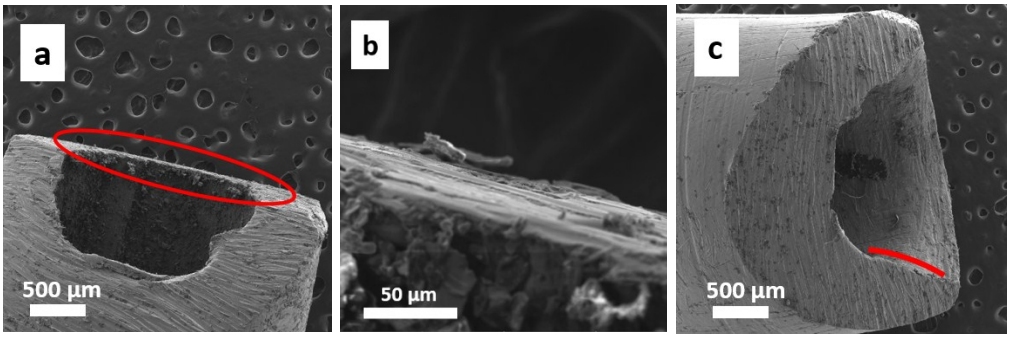

Fig. 3S. SEM images of (a) the inner edge of outlet, (b) magnified image of the inner edge, and (c) smoothed inner edge of outlet. For the convenience of SEM observation, the outlet was cut off half horizontally.

Table S1. Comparison of the operating conditions, graphene concentrations, length, thickness/layers, and Raman I_D/I_G ratio among the reported mechanical exfoliation methods and the gas-driven exfoliation method.

Reference	Methods	Operating conditions	Graphene concentrations	Length	Thickness/ layers	Raman I_D/I_G
This study	gas-driven	< 0.5 MPa	0.87 mg/ml	average 1.5 μm	1.1 nm	0.13
Chen et al. Chem. Commun. 2012, 48, 3703–3075	vortex	7000 rpm	-	-	-	-
Wahid et al. Green Chem. 2013, 15, 650	vortex	7000 rpm	-	-	-	-
Shen et al. Nanotechnology 2011, 22, 365306	jet cavitation	20 MPa	-	several hundred nanometers	1-2 nm	0.2-0.5
Liang et al. RSC Adv. 2014, 4, 16127	jet cavitation	30 MPa	0.05 mg/ml	-	1–1.5 nm	0.38
Yi et al. Chin. Sci. Bull. 2014, 59, 1794–1799	jet cavitation	45 MPa	-	0.65 μm^2	0.9 nm	-
Liang et al. J. Nanosci. Nanotechnol. 2015, 15, 2686–2694	jet cavitation	20 MPa	0.12 mg/ml	85% < 1 μm^2	1.3 nm	0.277
Yi et al. Carbon 2014, 78, 622–626	shear force	5000 rpm	0.22 mg/ml	-	-	<0.12
Paton et al. Nature Mater. 2014, 13, 624–630	shear force	4500 rpm	0.07 mg/ml	0.3-0.8 μm	5-8 layers	0.17-0.37
Liu et al. RSC Adv. 2014, 4:36464	shear force	9500 rpm	0.27 mg/ml	0.35-0.9 μm	2 nm	0.14-0.18
Varrla et al. Nanoscale 2014, 6, 11810–11819	shear force	18000 rpm	**1 mg/ml**	0.63 μm	6 layers	0.3-0.7
Xu et al. Carbon 2018, 135, 180–186	shear force	1000 rpm	0.0576 mg/ml	0.35 μm	0.6-1.0 nm	0.25-0.63
Nacken et al. Nature Mater. 2014, 13, 624–630	homogenizer	53 Mpa	0.223 mg/ml	0.02-0.58 μm	3 layers	0.52-0.78
Arao et al. Carbon 2017, 118, 18–24	homogenizer	35-43 Mpa	-	0.31 μm	-	0.24
Arao et al. Carbon 2016, 102, 330–38	homogenizer	50 Mpa	**7 mg/ml**	1.41 μm	4.07 layers	0.2
Zhao et al. J. Mater. Chem. 2010, 20, 5817–19	ball milling	300 rpm	-	-	0.8-1.8 nm	0.34
Hernandez et al. Nature Nanotech. 2008, 3:563–68	sonication	-	0.01 mg/ml	-	<5 layers	-
Bourlinos et al. Small 2009, 5, 1841–45	sonication	135 W	0.1 mg/ml	-	0.5-1 nm	-

Qian et al. Nano Res. 2009, 2, 706–12	sonication	-	10 wt%-12 wt%	0.1-0.8 μm	0.5-1.2 nm	≈0
Smith et al. New J. Phys. 2010, 12, 125008	sonication	75% of 750W	0.011-0.026 mg/ml	0.75 μm	4 layers	0.25-0.6
Khan et al. Small 2010, 6, 864–71.	sonication	25 W	**1.2 mg/ml**	1 μm	-	>0.2
Lotya et al.ACS Nano 2010, 4, 3155–62	sonication	80 W	0.3 mg/ml	0.5-1.2 μm	3.5-5 layers	0.57
Hernandez et al. Langmuir, 2010, 26, 3208–13	sonication	-	~0.08 mg/ml	-	2.5 layers	-
Wang et al. Chem. Commun. 2010, 46, 4487–89	sonication	80% of 750W	0.95 mg/ml	-	<5 layers	0.05-0.17
Arlene et al. J. Phy. Chem. C 2011, 115, 5422–28	sonication	16 W	0.5 mg/ml	1.1 μm	3.2 layers	0.208
Khan et al. Langmuir 2011, 27, 9077–9082	sonication	25% of 600W	63 mg/ml	1 μm	4.5 layers	0.2
Guardia et al. Carbon 2011, 49, 1653–1662	sonication	-	**1 mg/ml**	-	1.7 nm	0.53
Khan et al. Carbon, 2012, 50, 470–475	sonication	48 W	0.45 mg/ml	1.1 μm	2.6 layers	0.2
Zhou et al. Int. J. Electrochem. Sci. 2014, 9, 810–20	sonication	250 W	5% yield	1 μm	1 nm	0.33
Zhu et al. Mater. Chem. Phy. 2013, 137, 984–90	sonication	20% of 400W	-	2 μm	2.7 nm	0.49
Ramalingam et al. RSC Adv. 2013, 3, 2369	sonication	120 W	**2.28 mg/ml**	0.1 μm	1.5 nm	2
Bracamonte et al. J. Phy. Chem. C 2014, 118,15455–59	sonication	80 W	＞0.1 mg/ml	0.2-2 μm	-	>0.25
Carrasco et al. Carbon 2014, 70, 157–163.	sonication	75% of -	**1.08 mg/ml**	-	75% 0.9±0.2 nm	-
Wang et al. RSC Adv. 2016, 6, 56705	sonication	100 W	-	46.83 μm^2	1-3 nm	-
Liu et al. Carbon 2015, 83, 188–97	sonication	60% of 750W	0.65 mg/ml	<2 μm	-	0.45
Chen et al. Carbon 2015, 94, 405–11	sonication	5 W/ml	**6.5 mg/ml**	several microns	33.5% 1-2 layers	-
Cui et al. Carbon 2016, 99, 249–60	sonication	40 W	**3.25 mg/ml**	0.5-5 μm	1.1-2.9 nm	0.23
Manna et al. Carbon 2016, 105, 551–55	sonication	100 W	0.43 mg/ml	0.5-2 μm	-	0.51
Wang et al. Carbon 2018, 129, 191–98	sonication	20 W	**2.7 mg/ml**	2-10 μm	-	-
Karagiannidis et al. ACS Nano. 2017, 11, 2742–55	homogenizer	207 MPa	**100 mg/ml**	1 μm	12 nm	3.2
Paton et al. Mater. Res. Express 2017, 4, 025604	homogenizer	216 MPa	0.31 mg/ml	1.43 μm	12.9 layers	-

References

[1] Siddiqui, S. W.; Zhao, Y.; Kukukova, A.; Kresta, S. M. Characteristics of a Confined Impinging Jet Reactor: Energy Dissipation, Homogeneous and Heterogeneous Reaction Products, and Effect of Unequal Flow. Ind. Eng. Chem. Res. 2009, 48, 7945−7958.

[2] Panagiotis G. K.; Stephen A. H.; Lucia L.; et al. Microfluidization of Graphite and Formulation of Graphene-Based Conductive Inks. ACS Nano 2017, 11, 2742−2755.

[3] Boxall, J. A.; Koh, C. A.; Sloan, E. D.; et al. Droplet Size Scaling of Water-in-Oil Emulsions under Turbulent Flow. Langmuir 2012, 28, 104−110.